

Computer simulation of the heating sensor PIR detector by radiation

R. Drga, D. Janáčková, and H. Charvátová

Abstract—The work is focused on testing the sensors of security systems in the infrared region and its application in the security industry. To determine the behaviour of PIR detector, it was necessary to design a mathematical model of heat sensor and sensor simulation of the thermal behaviour in the environment COMSOL Multiphysics, with subsequent verification of the proposed mathematical model. The theoretical conclusions of a mathematical description enabled the subsequent implementation of laboratory workplace of IR radiation for specific measurement properties of light sources and sensors, where it is also possible to measure the spatial characteristics of PIR detectors.

Keywords—PIR detector, pyroelement, radiation, mathematical model.

I. INTRODUCTION

THIS work deals with the testing of sensors of security systems in the field of infrared radiation and its use in the security industry, the output of work may also be used in courses technical means security industry, electronic security systems, which are the subjects of teaching at the Department of Security Engineering, Faculty of Applied Informatics, University of Tomas Bata University in Zlín. The work is focused mainly on the PIR detectors, which are used most widely in security technologies. For thermal balance PIR detector and pyroelement was necessary to design a mathematical model described below and perform simulations of the thermal behavior of the sensors in the environment of COMSOL Multiphysics to verify the accuracy of the measurement pyroelement time close to zero at low density thermal radiation.

This work was supported by the European Regional Development Fund under the project CEBIA-Tech No. CZ.1.05/2.1.00/03.0089.

R. Drga, Tomas Bata University in Zlín, Faculty of Applied Informatics, Department of Security Engineering, nám. T. G. Masaryka 5555, 760 01 Zlín, Czech Republic (e-mail: rdrga@fai.utb.cz)

D. Janáčková, Tomas Bata University in Zlín, Faculty of Applied Informatics, Department of Automation and Control Engineering, nám. T. G. Masaryka 5555, 760 01 Zlín, Czech Republic (e-mail: janacova@fai.utb.cz)

H. Charvátová, Tomas Bata University in Zlín, Faculty of Applied Informatics, Department of Automation and Control Engineering, nám. T. G. Masaryka 5555, 760 01 Zlín, Czech Republic (e-mail: charvatova@fai.utb.cz)

II. MATHEMATICAL MODEL OF HEATING SENSOR BY RADIATION

As a module we used the room heated by two heat sources, as you can see in Fig1.

Thermal radiation incident on the sensor is partially reflected and some is absorbed by the sensor, thereby to ensure that the temperature measured at the beginning of the measurement does not fully effective temperature.

For the quantitative description of the temperature distribution in the heated pyroelement radiation we used the Stefan-Boltzmann law, according to which the density of heat flow between the source and the heated surface expressed as (1) [3]:

$$q(\tau) = \sigma \cdot C(T_2^4 - T_1^4) \quad (1)$$

where:

σ - Stefan-Boltzmann constant

C - emission surface and geometric properties, [1]

T_2 - source temperature, [K]

T_1 - temperature of heated surface, in this case the surface temperature, [K]

$$\frac{\partial T}{\partial \tau} = a \cdot \frac{\partial^2 T}{\partial x^2}, \quad (0 < x < b, 0 < \tau) \quad (2)$$

$$\left(\frac{\partial T}{\partial x} \right)_{x=0} = 0 \quad (3)$$

$$\lambda \left(\frac{\partial T}{\partial x} \right)_{x=b} = q \quad (4)$$

$$T = T_p \quad \text{for} \quad \tau = 0 \quad (5)$$

where:

b - half the thickness of the sensor, [m]

x - direction coordinates, [m]

Laplace transform of equation (1) with conditions (2) to (5) has been obtained analytical solution of unsteady temperature field for symmetrically heated by radiation sensor plate shape:

$$\frac{T - T_p}{T_c - T_p} = K_i \left[Fo + \frac{1}{2} \left(\frac{x}{b} \right)^2 - \frac{1}{6} - 2 \sum_{n=1}^{\infty} \frac{\cos \left(\frac{x}{b} p_n \right)}{p_n^2 \cos p_n} e^{(-Fop_n^2)} \right] \quad (6)$$

where K_i is Kirpičev criterion (7)

$$K_i = \frac{qb}{\lambda(T_c - T_p)} \quad (7)$$

where T_c is medium temperature of radiators. Fourier criterion Fo represents the dimensionless heating time is calculated by the equation:

$$Fo = \frac{a\tau}{b^2} \quad (8)$$

where:

τ - duration of heating, [s]

a - thermal conductivity sensor, [$m^2 \cdot s^{-1}$]:

$$a = \frac{\lambda}{\rho c_p} \quad (9)$$

where:

λ - the thermal conductivity sensor, [$W \cdot m^{-1} \cdot K^{-1}$]

ρ - the density of the sensor material, [$kg \cdot m^{-3}$]

c_p - the specific heat capacity of the sensor material, [$J \cdot kg^{-1} \cdot K^{-1}$].

Members p of the analytical solution of (6) are determined from equation (10):

$$p_n = n \cdot \pi \quad (10)$$

According to the form the solution (6) it is evident that with increasing time of heating effect element endless series decreases, i.e., we can also expect Fourier criterion Fo which influence endless series may be neglected and $Fo > Fok$ the temperature at any point in the wall almost linear function time and temperature profile across the plate (x -axis direction) is a parabola.

III. SOLUTION OF A MATHEMATICAL MODEL IN THE MAPLE ENVIRONMENT

Solution temperature distribution in pyroelement according to equation (6) was performed using the software applications created in Maple environment. To this purpose, the program created an application that performs automatic calculation of temperature fields for the specified input value. The source code is as follows:

Defining input values:

```
> q:=1;
> b:=0.005;
> lambda:=4.6;
> tc:=36;
> tp:=20;
> rho1:=7450;
```

```
> cp:=250;
> a:=lambda/(rho1*cp);
> Fo:=a*tau/b^2;
```

The calculation of the roots of p:

```
> for i from 1 to 300 do
p[i]:=evalf(Pi*i)
end do;
```

```
p1 := 3.141592654
p2 := 6.283185308
p3 := 9.424777962
⋮
```

Calculation of 3D temperature field based on the analytical solution (6):

```
> with(plots):
> grafreal:=plot3d((q/lambda*(a*tau/b+x^2/(2*b)-
(b/6))-2*q*b/lambda*Sum(cos(x/b*p[n])*exp(-
(a*tau/b^2)*p[n]^2)/(p[n]^2*cos(p[n])),n=1..300))+tp
,x=0..b,tau=0..60,axes=box,style=wireframe,color=red
,labels=["x (m)", "tau (s)", "t (degC)"]);
> display(grafreal);
```

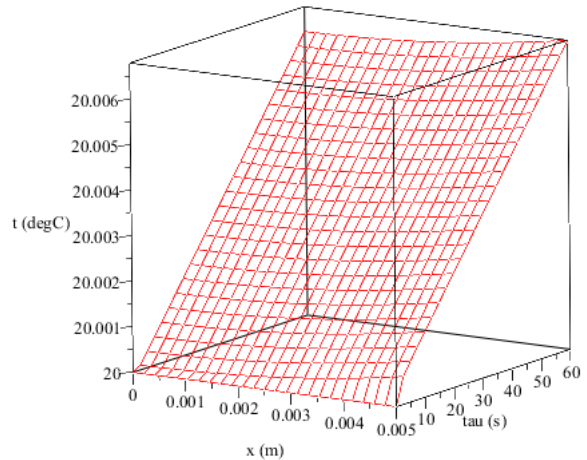


Fig. 1 3D temperature field in a heated sensor calculated in Maple

Calculation of temperature fields in 2D on the basis of analytical solutions (6):

```
> for j from 1 to 10 do
fce2D[j]:=q/lambda*(a*tau[j]/b+x^2/(2*b)-(b/6))-
2*b/lambda*Sum(cos(x/b*p[n])*exp(-
(a*tau[j]/b^2)*p[n]^2)/(p[n]^2*cos(p[n])),n=1..300)+tp
end do;
> for k from 1 to 10 do
tau[k]:=6*k
end do;
tau1 := 6
tau2 := 12
tau3 := 18
⋮
```

```
>graf1:=plot(fce2D[1],x=0..b,legend=tau[1],axes=box,color=
COLOR(HUE, .1));

>graf2:=plot(fce2D[2],x=0..b,legend=tau[2],axes=box,color=
COLOR(HUE, .2));

>graf3:=plot(fce2D[3],x=0..b,legend=tau[3],axes=box,color=
COLOR(HUE, .3));
:
:
>display(graf1,graf2,graf3,graf4,graf5,graf6,graf7,graf8,graf9,
graf10);
```

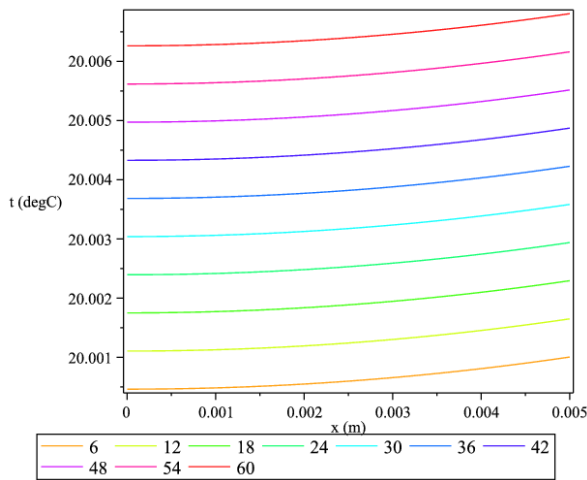


Fig. 2 3D temperature field in a heated sensor calculated in Maple

Calculation of the temperature sensor in the desired location and time:

```
> x[zvol]:=0.002;
    x_zvol := 0.002
> tau[zvol]:=550;
    tau_zvol := 550

>evalf((q/lambda*(a*tau[zvol]/b+x[zvol]^2/(2*b)-(b/6))-
2*b/lambda*Sum(cos(x[zvol]/b*p[n])*exp(-
(a*tau[zvol]/b^2)*p[n]^2)/(p[n]^2*cos(p[n])),n=1..300)+tp)
);
    20.05898920
```

The output of the program application is a plot showing the 3D and 2D real temperature field in a heated sensor to the desired input value. 3D temperature field shows the temperature distribution for a selected period of heating sensor (Fig. 1). 2D temperature field shows the temperature curve of the sensor at the desired times of heating (Fig. 2). The application also calculates the temperature of sensor in a given place and time, as shown in the last part of the above source file.

IV. SIMULATION AND VERIFICATION PROPOSED MODELS IN COMSOL MULTIPHYSICS

Because it was not possible to determine experimentally the necessary data, was used to assess the thermal behavior of the sensor software COMSOL Multiphysics, which is suitable for the simulation of physical processes and is intended primarily for developers, researchers and researchers. The aim of simulation is to determine the temperature distribution and the heat flow density in the surface of the pyroelectric element location depending on the distance from the intruder detector. The "Heat Transfer Module" was used for the simulation, for environment "Surphace-to-Surphace Radiation". Size intruder simulating the glowing area of 2 m x 0.5 m, the properties of the detector represents pyroelement of size 5 mm x 2.3 mm x 0.2 mm. The simulation was performed under the conditions:

- the surface temperature of an intruder 36 °C
- ambient air temperature 20 °C
- relative emissivity of the surface of a pyroelectric element 0.9
- relative emissivity of 0.97 intruder
- thermal conductivity of the pyroelectric element $2,255 \cdot 10^{-6} \text{ m}^2/\text{s}$
- thermal conductivity intruder $1,484 \cdot 10^{-7} \text{ m}^2/\text{s}$
- thermal conductivity of air $2,14 \cdot 10^{-5} \text{ m}^2/\text{s}$

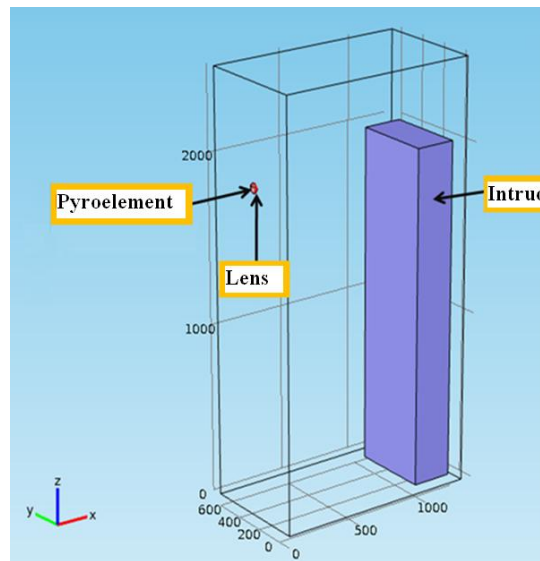


Fig. 3 The geometric layout of the situation

The following pictures show the simulation results, ie, temperature distribution and heat flow density at the surface of the pyroelectric element spot for intruder distance of 1 m from the detector. Similarly, simulations were performed for a distance of 3 and 5 m

According to Figure 5 it is apparent that near pyroelementu leads to increase in air temperature due to the temperature at a greater distance from the detector.

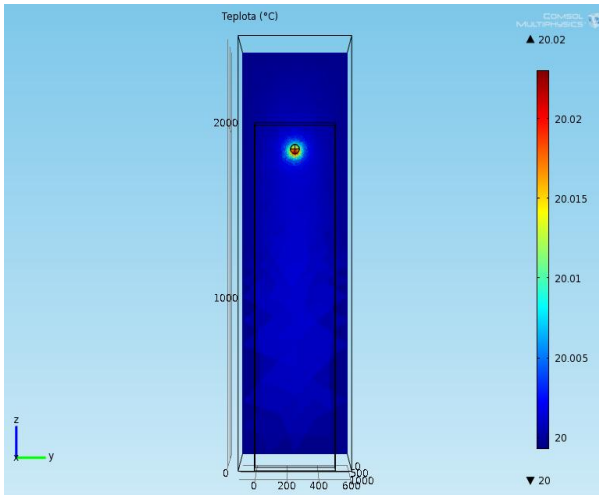


Fig. 4 The temperature distribution in the cross-sectional surface at the site of a pyroelectric element

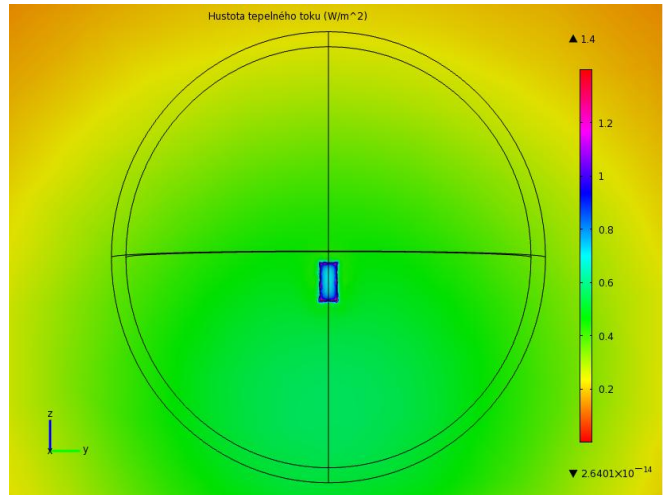


Fig. 7 The distribution density of the heat flow at the site of the cut surface of the pyroelectric element - detail in the place of the detector

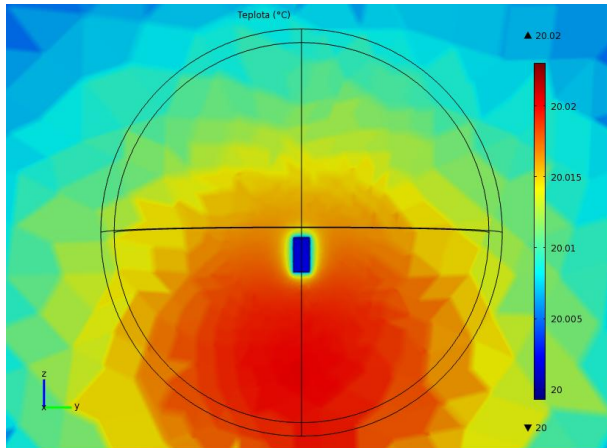


Fig. 5 The temperature distribution in the cut surface at the point a pyroelectric element - detail in location of the detector

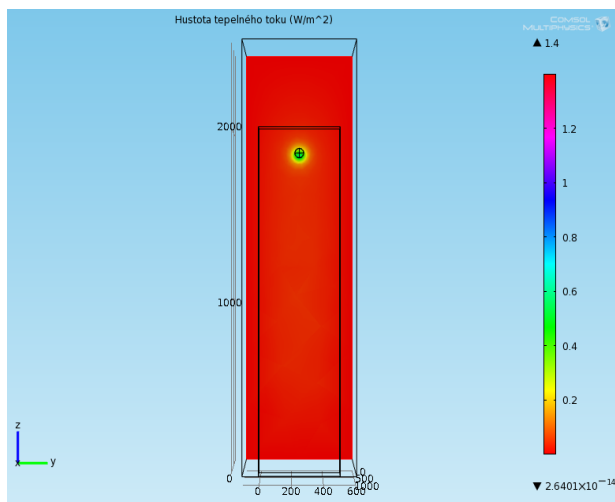


Fig. 6 The temperature distribution in the cut surface at the site of a pyroelectric element - detail the location of the detector

Figure 7 is then detail the distribution of heat flow density in the vicinity pyroelementu. Near pyroelementu density of heat flow increases until it reaches about 0.5 W/m^2 higher relative to the surroundings.

In the case of an intruder detector distance 3 m decreased heat flow density to approximately 0.24 W/m^2 , while a further decrease of the surface temperature pyroelement.

Specified the value of the density of heat flow and temperature at the surface pyroelement according to the results of simulation in COMSOL Multiphysics is detailed in the following table. These values correspond to the mid-position of the element.

Table I Heat flux density on the surface of the pyroelectric element - the results of simulation in COMSOL Multiphysics

Distance detector from intruder [m]	Heat density [W/m ²]	Temperature [°C]
1	0,750	20,0230
2	0,380	20,0076
3	0,245	20,0012
4	0,035	20,0010
5	0,020	20,0004

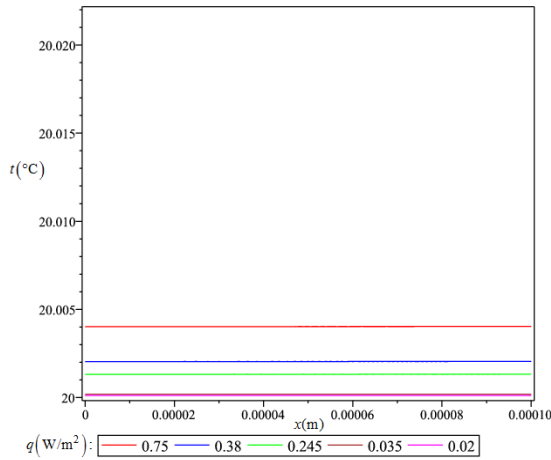
The table shows that with increasing distance decreases heat flow density on the surface of the original pyroelement 0.75 W/m^2 at 0.02 W/m^2 . It also reduces the surface temperature pyroelement value of 20.023 °C at 20.0004 °C .

V. CALCULATION OF TEMPERATURE FIELDS IN MAPLE

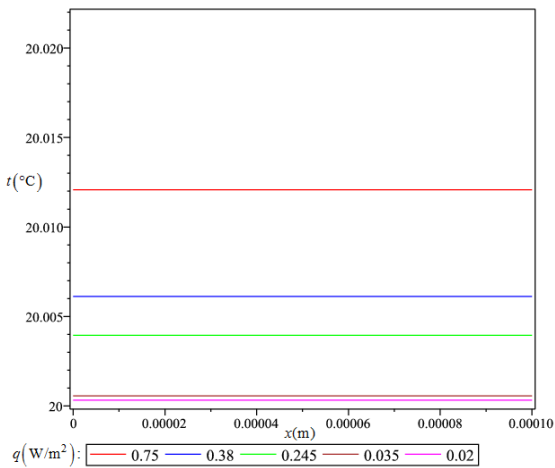
The density of heat flow, obtained by simulation in COMSOL Multiphysics is used for the calculation of unsteady temperature fields in pyroelement according to the analytical solution (6) model (2) - (5). For the calculation of temperature fields were used the following values:

element thickness 0.2 mm
 initial temperature of the pyroelectric element 20 °C
 surface temperature of the intruder (source) 36 °C

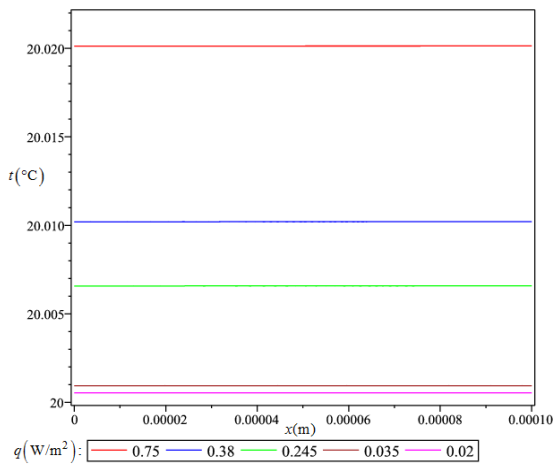
The following pictures show waveforms of temperature on the surface pyroelement in terms of heat flow density from 0.75 W/m² to 0.02 W/m², which corresponds to the distance from the intruder detector 1 m to 5 m.



The duration of heat exposure: 1 second



The duration of heat exposure: 3 seconds



The duration of heat exposure: 5 second

Fig. 8 The course of the temperature field in pyroelement depending on the density of heat flux at the surface of the element

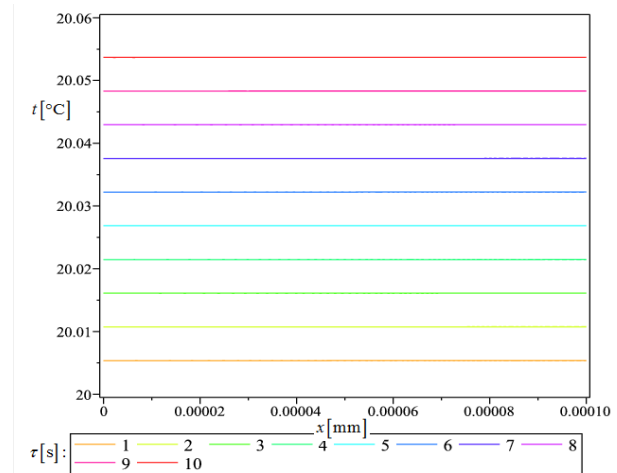
From the graphs it is evident that the heat treatment for 1-5 seconds for incident radiation having a density of 0.75 W/m² temperature pyroelement increased about 0.015 °C, while for incident radiation having a density of 0.02 W/m², the temperature hardly increased pyroelement. The calculations and simulations, the temperature distribution in the heated pyroelement also shows that even at low values of the density of heat flux at a given time, the surface temperature pyroelement nearly the same temperature throughout its thickness (no steep temperature field). This proves that pyroelement is flawed. It can be said that in the early stages of measurement evaluates pyroelement right temperature and laboratory measurements is therefore in the initial stages sufficiently accurate.

VI. COMPARISON OF THEORETICAL RESULTS WITH SIMULATIONS

Verification of the mathematical model was made by comparing the temperature fields in pyroelement calculated in the Maple on the basis of the analytical solution described by equation (6) with the results of the simulation of temperature field in COMSOL Multiphysics.

The Figure 9 shows the waveforms of temperature fields under the following conditions:

- secondary source temperature 30° C
- initial temperature pyroelement 20 °C
- the density of heat flux incident on a surface pyroelement 1 W/m²
- thermal conductivity pyroelement 2,255.10⁻⁶ m²/s,
- pyroelement thickness of 0.2 mm.



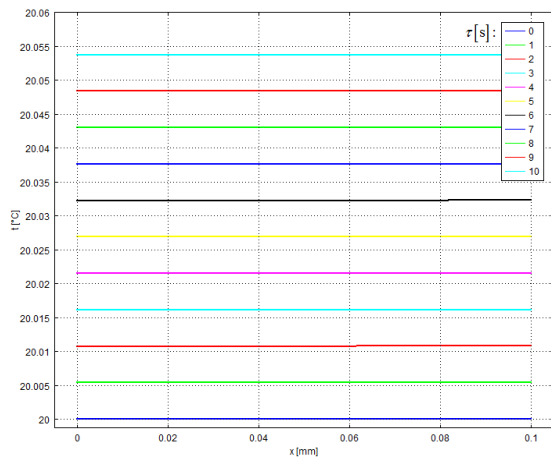


Fig. 9 Temperature field in pyroelement for the heat of the action 10 seconds calculated in Maple (up) and COMSOL Multiphysics (down)

It is evident that the curves of temperature fields calculated in Maple coincide with the courses of temperature fields obtained by simulation in COMSOL Multiphysics.

VII. CONCLUSION

Analytical solution of the proposed mathematical model describing heat radiation sensor was used to create applications for the calculation of temperature fields in pyroelement in the user interface of the program Maple. Because it was not possible to determine all the data needed for the calculation of temperature fields experimentation was conducted simulations to assess the thermal behavior pyroelement programming environment COMSOL Multiphysics. The simulations were designed waveforms temperature fields and heat flux density at the surface and under surface pyroelement for the selected distance from the intruder detector. The data obtained were then compared with the theoretical results obtained by the solution of the model through an application program created in Maple environment. The calculations and simulations, the temperature distribution in the heated pyroelement showed that even at low values of heat flow density in a given time the surface temperature pyroelement nearly the same temperature throughout its thickness, which confirmed that in the early stages of measurement evaluates pyroelement right temperature and laboratory measurements is therefore in the initial stages is sufficiently accurate.

Based on the theoretical results and the mathematical description was later realized laboratory workplace interior IR radiation, which was made specific measurements of the properties of radiation sources and detectors, and where it is also possible to measure the spatial characteristics PIR detectors.

REFERENCES

- [1] J. D. Vincent, *Fundamentals of infrared detector operation and testing*. USA, Texas: WILEY, 1990.
- [2] G. F. Knoll, *Radiation detection and measurement*. USA, Texas: WILEY, 2000.
- [3] B. Saleh, *Fundamentals of photonics*. USA, Texas: WILEY, 2007.
- [4] K. Kolomazník, *Teorie technologických procesů III*. (in Czech). University of Technology in Brno, Brno, 1978
- [5] A., R. Jha, . *Infrared technology*. USA – Texas: WILEY, 2006
- [6] C. Hotz, *Přenos tepla zářením* (in Czech), Prague: SNTL, 1979.
- [7] K. Kolomazník, *Modelování zpracovatelských procesů* (in Czech), Brno: University of Technology in Brno, 1990.
- [8] K. Židek and J. Pítel, "Smart 3D Pointing Device Based on MEMS Sensor and Bluetooth Low Energy," in *Proceedings of the 2013 IEEE Symposium on Computational Intelligence in Control and Automation (CICA)*, Singapore, April 16-19, 2013, pp. 165-168.
- [9] R. Makovník and O. Liška, "Contribution to experimental identification and simulation problems of dynamic systems", *Ovidius University Annual Scientific Journal*. vol. 9, No. 1, 2007.
- [10] O. Liška (2008). Monitorizačné systémy pre automatizovanú výrobu (in Slovak). *Transfer inovácií*. [Online]. 12. pp. 121-123. Available: <http://www.sjf.tuke.sk/>
- [11] M. Fodor, O. Liška (2010). Design and realization sensorial system on detection obstacle [CD-ROM].in *8th International Symposium on Applied Machine Intelligence and Informatics*, Herľany, Slovakia.